

hSNMF: HYBRID SPATIALLY REGULARIZED NMF FOR IMAGE-DERIVED SPATIAL TRANSCRIPTOMICS

Md Ishtyaq Mahmud^{}1 Veena Kochat^{*}2 Suresh Satpati² Jagan Mohan Reddy Dwarampudi¹
 Humaira Anzum¹ Kunal Rai^{†2} Tania Banerjee^{‡31}*

¹ Department of Electrical and Computer Engineering, University of Houston

² Department of Genomic Medicine and MDACC Epigenomics Therapy Initiative (METI),
 MD Anderson Cancer Center, Houston TX, USA

³ Department of Information Science Technology, University of Houston, Houston, TX, USA

ABSTRACT

High-resolution spatial transcriptomics platforms, such as Xenium, generate single-cell images that capture both molecular and spatial context, but their extremely high dimensionality poses major challenges for representation learning and clustering. In this study, we analyze data from the Xenium platform, which captures high-resolution images of tumor microarray (TMA) tissues and converts them into cell-by-gene matrices suitable for computational analysis. We benchmark and extend nonnegative matrix factorization (NMF) for spatial transcriptomics by introducing two spatially regularized variants. First, we propose Spatial NMF (SNMF), a lightweight baseline that enforces local spatial smoothness by diffusing each cell's NMF factor vector over its spatial neighborhood. Second, we introduce Hybrid Spatial NMF (hSNMF), which performs spatially regularized NMF followed by Leiden clustering on a *hybrid adjacency* that integrates spatial proximity (via a contact–radius graph) and transcriptomic similarity through a tunable mixing parameter α . Evaluated on a cholangiocarcinoma dataset, SNMF and hSNMF achieve markedly improved spatial compactness ($\text{CHAOS} < 0.004$, Moran's $I > 0.96$), greater cluster separability (Silhouette > 0.12 , DBI < 1.8), and higher biological coherence (CMC and enrichment) compared to other spatial baselines. **Availability and implementation:** <https://github.com/ishtyaqmahmud/hSNMF>

1. INTRODUCTION

High-resolution spatial transcriptomics (ST) technologies, exemplified by the Xenium platform (10x Genomics), have emerged as transformative tools in genomics [1], [2]. By capturing gene expression profiles at single-cell resolution while preserving native spatial coordinates, these assays enable unprecedented analysis of tissue microenvironments, and spatial

organization in complex diseases[3, 4]. However, the resulting data are extremely high-dimensional and sparse, posing major computational challenges [5]. As in single-cell RNA sequencing (scRNA-seq), effective dimensionality reduction (DR) is critical to reveal cellular subpopulations[6]. Because ST integrates quantitative imaging with high-throughput genomics, advances in this area demand the same methodological rigor that has driven progress in biomedical image analysis: precise signal extraction, robust dimensionality reduction, and interpretable feature representations. Consequently, enhancing spatial interpretability and scalability enables data-driven insights into tissue structure and disease pathology at single-cell resolution [7, 8].

Standard DR methods such as Principal Component Analysis (PCA) and Non-negative Matrix Factorization (NMF) [9] treat each cell as an independent sample, ignoring spatial context. This “a-spatial” assumption often produces fragmented, “salt-and-pepper” clusterings that are biologically incoherent and fail to capture continuous tissue structures. To address this limitation, spatially aware DR methods have been developed. Broadly, these approaches fall into two major families:

1. **Probabilistic Models**, such as Nonnegative Spatial Factorization (NSF) [10], which use Gaussian Processes to model spatial correlation. While powerful, these models are computationally intensive and scale poorly with the large cell counts generated by modern platforms like Xenium.
2. **Filter-based Methods**, including Randomized Spatial PCA (RASP) [11] and our baseline Spatial NMF (SNMF), which first learn an a-spatial embedding (e.g., via NMF) and then smooth it using a spatial graph. These are efficient and scalable but often rely on oversimplified k-nearest neighbor (k-NN) topologies that fail to reflect true physical proximity or multi-scale tissue structure.

Deep learning-based approaches such as graph neural networks (GNNs) have also been proposed, but their latent embeddings are often opaque and less interpretable for biological analysis [12], [13].

^{*} Core contributors, [†] Joint advising

Correspondence to: tbanerjee@uh.edu, krai@mdanderson.org

This work introduces two spatially aware extensions of NMF for dimensionality reduction in spatial transcriptomics. The key contributions of the paper may be summarized as:

1. We present Spatial NMF (SNMF), a lightweight two-stage baseline that enhances standard NMF embeddings through spatial smoothing of cell factors over local neighborhoods, providing an interpretable bridge between expression-based and spatially informed analyses.
2. We further propose Hybrid Spatial NMF (hSNMF), which performs spatially regularized NMF followed by Leiden clustering on a *hybrid adjacency* that combines spatial proximity and transcriptomic similarity. The spatial component employs a contact–radius graph that merges short-range contact edges with longer-range contextual connections, allowing hSNMF to jointly optimize geometric contiguity and molecular coherence.

Together, SNMF and hSNMF offer parameter-efficient, interpretable, and scalable baselines for capturing spatial organization in high-dimensional gene expression data.

2. METHODOLOGY

2.1. Dataset and Preprocessing

We used the same Xenium spatial transcriptomics (ST) dataset and initial preprocessing pipeline described in our prior work [14], with additional steps to construct spatial graphs for the proposed SNMF and hSNMF models. Briefly, the dataset consists of $N = 25$ cholangiocarcinoma patients (total of $M = 40$ tumor microarray cores) profiled on the Xenium platform using a 480-gene target panel, yielding $\approx 212,000$ cells. Each core produced high-resolution tissue images that were processed to generate single-cell expression matrices and spatial coordinates. All samples were anonymized TMAAs obtained from the MD Anderson Cancer Center, representing intrahepatic cholangiocarcinoma resections.

1. *Quality control (QC) and gene filtering.* Genes detected in fewer than three cells and cells with fewer than 200 detected genes (including negative-control probes) were removed. Doublet detection was performed with Scrublet following Wolock et al. [15], and cells with doublet scores >0.2 were excluded. After QC, 191,125 high-confidence single-cell profiles remained.
2. *Normalization and transformation.* Counts were normalized per cell to 10,000 total counts and log-transformed as $\log_e(x+1)$.
3. *Spatial encoding.* Each cell’s centroid (x, y) was extracted from the Xenium metadata and used to build spatial graphs. Specifically, we constructed both a short-range **contact graph** (radius = 20 μm) and a broader **radius graph** (radius = 80 μm), later combined into a hybrid adjacency for spatial smoothing and clustering.

2.2. Existing Spatial Dimensionality Reduction Methods

To evaluate the performance of our proposed hSNMF framework, we conducted a comparative analysis against several state-of-the-art methods. These methods utilize different underlying technologies, including PCA and matrix factorization.

RASP (Randomized Spatial PCA) [11]: RASP is a spatially aware dimensionality reduction method optimized for large-scale ST data. Built on a randomized two-stage PCA framework with sparse matrix operations, it achieves high computational efficiency and scales to hundreds of thousands of spatial locations. A configurable spatial smoothing step integrates spatial context, enabling de-noised expression reconstruction and flexible inclusion of non-transcriptomic covariates.

NSF (Nonnegative Spatial Factorization) [10]: NSF is a spatially aware probabilistic model that extends NMF by placing Gaussian Process priors on latent factors, enforcing spatial smoothness. Gene counts are modeled with non-negative loadings under Poisson or Negative Binomial likelihoods, producing sparse, interpretable components. A hybrid variant (NSFH) combines spatial and nonspatial factors to quantify gene-level spatial effects.

2.3. Proposed Spatial Extensions of NMF

Spatial NMF (SNMF). We introduce *Spatial NMF (SNMF)* as a lightweight two-stage baseline that incorporates spatial context into standard nonnegative matrix factorization (NMF).

Given the log-normalized cell-by-gene expression matrix $\mathbf{X} \in \mathbb{R}_{\geq 0}^{n \times p}$, we first compute nonnegative latent factors $\mathbf{W} \in \mathbb{R}_{\geq 0}^{n \times k}$ and $\mathbf{H} \in \mathbb{R}_{\geq 0}^{k \times p}$ by solving

$$\min_{\mathbf{W}, \mathbf{H} \geq 0} \|\mathbf{X} - \mathbf{WH}\|_F^2. \quad (1)$$

To encourage spatial smoothness, we apply a single-step post hoc averaging to the latent representation. Specifically, each cell’s factor vector \mathbf{w}_i is replaced by the average of its $k = 15$ nearest spatial neighbors:

$$\mathbf{w}'_i = \frac{1}{|\mathcal{N}_S(i)|} \sum_{j \in \mathcal{N}_S(i)} \mathbf{w}_j, \quad (2)$$

where $\mathcal{N}_S(i)$ denotes the spatial neighborhood of cell i . This local averaging acts as a low-pass filter on the latent space, yielding a smoothed embedding \mathbf{W}' that is used for downstream clustering.

SNMF is included as a conceptual baseline to illustrate the effect of simple spatial smoothing on NMF embeddings; however, we focus our empirical evaluation on hSNMF, which consistently outperformed SNMF in preliminary analyses.

Table 1: Pareto-optimal hyperparameter settings per method and their performance metrics.

Method	k	ρ	Clusters	CHAOS \downarrow	Moran's I \uparrow	Silhouette \uparrow	DBI \downarrow	CMC \uparrow	MER \downarrow	Enrich. \uparrow
RASP	5	0.4	17	0.005	0.649	0.166	1.399	0.796	0.548	1.968
RASP	10	0.4	15	0.004	0.649	0.183	1.604	0.838	0.385	2.078
RASP	15	0.4	14	0.004	0.649	0.166	1.711	0.809	0.276	1.729
NSF	5	0.4	24	0.003	0.992	-0.879	2.043	0.580	0.934	1.475
NSF	5	0.6	29	0.003	0.992	-0.881	3.191	0.587	1.475	0.927
NSF	10	0.6	25	0.005	0.993	-0.585	5.857	0.521	1.764	0.954
SNMF	10	0.4	27	0.003	0.964	0.128	1.207	0.764	1.876	0.555
SNMF	10	0.8	39	0.003	0.964	0.153	1.335	0.762	1.957	0.586
SNMF	10	1	43	0.003	0.964	0.163	1.294	0.760	1.843	0.599
hSNMF	10	0.4	23	0.002	0.970	0.274	1.423	0.720	0.445	1.967
hSNMF	15	0.4	24	0.002	0.982	0.178	1.689	0.715	0.505	2.285
hSNMF	25	0.4	27	0.002	0.941	0.228	1.687	0.721	0.497	2.101
hSNMF	25	0.8	29	0.002	0.941	0.229	1.653	0.717	0.981	2.175

Hybrid Spatially Smoothed NMF (hSNMF). We next propose *Hybrid Spatially Smoothed NMF (hSNMF)*, which extends SNMF by applying iterative spatial diffusion over a hybrid spatial graph and integrating spatial and molecular similarity during clustering.

We begin with the same log-normalized expression matrix $\mathbf{X} \in \mathbb{R}_{\geq 0}^{n \times p}$ and factorize it using standard NMF with k components (`init=nndsvda`, `max_iter=500`, `random_state=0`):

$$\mathbf{X} \approx \mathbf{W}\mathbf{H}. \quad (3)$$

To incorporate spatial coherence, we construct a *hybrid spatial adjacency matrix* \mathbf{A}_s that combines contact-based edges within radius $r_c = 20 \mu\text{m}$ and radius-based edges within $r_r = 80 \mu\text{m}$, merged via maximum-weight selection to preserve local tissue structure. Let \mathbf{D} denote the degree matrix of $\mathbf{A}_s + \mathbf{I}$. We define a row-stochastic diffusion operator

$$\mathbf{P} = \mathbf{D}^{-1}(\mathbf{A}_s + \mathbf{I}). \quad (4)$$

Spatial smoothing is then applied to the latent factors through iterative diffusion:

$$\mathbf{W}^{(t+1)} = (1 - \beta) \mathbf{W}^{(t)} + \beta \mathbf{P} \mathbf{W}^{(t)}, \quad (5)$$

with $\beta = 0.8$ and two diffusion steps, producing the spatially smoothed embedding \mathbf{W}_s . To preserve nonnegativity, we clip any small numerical negatives in \mathbf{W}_s to zero.

Next, we construct a k_{nn} -nearest-neighbor graph \mathbf{A}_f in the smoothed latent space \mathbf{W}_s to capture transcriptional similarity ($k_{\text{nn}} = 15$). We then form a *dual-graph adjacency*

$$\mathbf{A}_{\text{mix}} = \alpha \mathbf{A}_s + (1 - \alpha) \mathbf{A}_f, \quad (6)$$

where $\alpha \in [0, 1]$ controls the trade-off between spatial proximity and molecular similarity ($\alpha = 0.5$ by default). All adjacency matrices are row-stochastic to ensure scale comparability.

Finally, Leiden clustering is applied directly to \mathbf{A}_{mix} to obtain communities that are both spatially contiguous and transcriptionally coherent. The resulting clusters are evaluated using spatial (CHAOS, Moran's I), geometric (Silhouette, DBI), and biological (Marker Fraction, MER, Enrichment) metrics.

3. EVALUATION METRICS

We quantitatively assessed the spatial quality of embeddings using two complementary metrics: CHAOS, which measures spatial compactness of discrete clusters, and Moran's I, which measures spatial autocorrelation of continuous latent factors.

CHAOS: Spatial Cluster Compactness: CHAOS quantifies how spatially cohesive each cluster is by computing the mean distance between each cell and its nearest same-cluster neighbor. Lower values indicate tighter, more spatially compact clusters. Given standardized (x, y) coordinates for all N cells, the CHAOS score is:

$$\text{CHAOS} = \frac{1}{N} \sum_{k \in K} \sum_{i \in C_k} \min_{j \in C_k, j \neq i} d(i, j),$$

where K is the set of clusters and C_k the set of cells in cluster k .

Moran's I: Spatial Autocorrelation: Moran's I measures the spatial correlation of continuous features (e.g., latent factors). For feature vector y and spatial weight matrix W , it is defined as:

$$I = \frac{N}{\sum_i \sum_j w_{ij}} \frac{\sum_i \sum_j w_{ij} (y_i - \bar{y})(y_j - \bar{y})}{\sum_i (y_i - \bar{y})^2},$$

where N is the number of cells, y_i the feature value for cell i , and w_{ij} the spatial weight (from a k -NN or radius graph). Values $I > 0$, $I < 0$, and $I \approx 0$ correspond to clustered, dispersed, and random spatial patterns, respectively. We compute I on the first latent factor of each embedding for cross-model comparison.

Other Metrics In addition to CHAOS and Moran's I, we also evaluate embeddings using several metrics defined by Mamud et. al in [14]: Silhouette Score, Davies–Bouldin Index (DBI), Cluster Marker Coherence (CMC), Marker Exclusion Rate (MER), and Marker Enrichment.

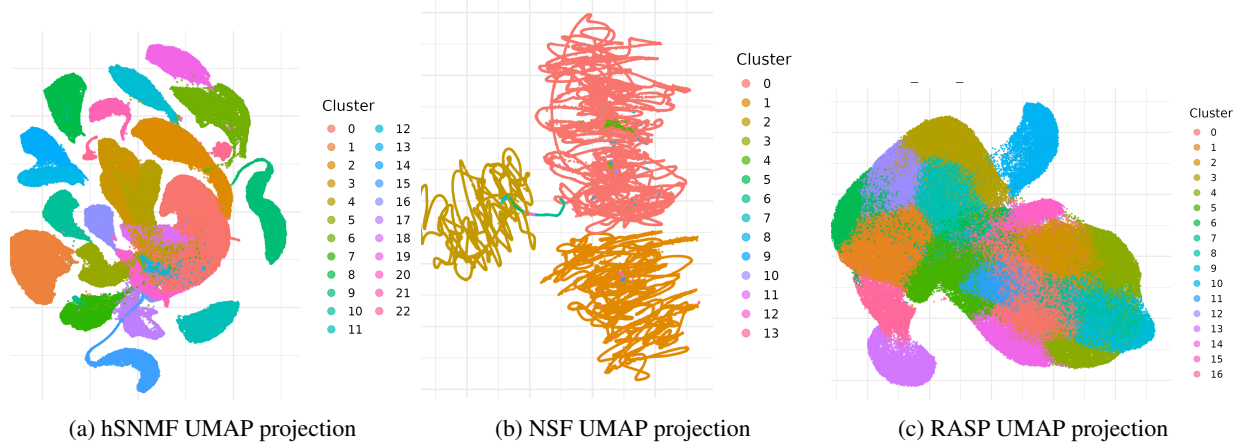


Fig. 1: UMAP projections of cell clusters obtained after applying Leiden clustering on the reduced cellxgene vectors.

4. RESULTS

4.1. Pareto-front Analysis

To systematically evaluate the performance trade-offs inherent in each spatial dimensionality reduction method, we performed a comprehensive grid search across key hyperparameters. For each method (RASP, NSF, SNMF, and hSNMF), we varied the latent dimensionality

$$k \in \{5, 10, 15, 20, 25, 30, 35, 40\}$$

and Leiden clustering resolution

$$\rho \in \{0.1, 0.2, 0.3, 0.4, 0.5, 0.6, 0.7, 0.8, 0.9, 1.0, 1.2\}.$$

At each (k, ρ) parameter combination, we evaluated the resulting embedding and clustering using the suite of quantitative metrics defined in Section 3. We then identified the Pareto-optimal (k, ρ) configurations for each method. The Pareto front, in our case, represents the set of hyperparameter settings for which no other setting simultaneously improves CHAOS, Moran’s I , Silhouette Scores, and DBI.

Table 1 summarizes the Pareto-optimal configurations and corresponding performance metrics for all evaluated spatial DR variants. The proposed spatial models, **SNMF** and **hSNMF**, consistently exhibit high spatial compactness (CHAOS < 0.004) and strong spatial autocorrelation (Moran’s $I \approx 0.96\text{--}0.98$), confirming effective spatial regularization. Unlike the NSF baseline, which yields negative Silhouette scores and poor cluster separability, SNMF and hSNMF achieve positive Silhouette values (0.15–0.27) with moderate Davies–Bouldin indices, indicating well-separated and cohesive clusters. hSNMF, which incorporates the contact–radius hybrid graph, further improves both Silhouette and enrichment while maintaining low MER and high CMC, thereby balancing spatial contiguity and molecular coherence. In contrast, the RASP baseline attains modest geometric performance but markedly lower Moran’s I , reflecting weaker spatial consistency. Overall, the hybrid hSNMF formulation

attains the most favorable trade-off among spatial smoothness, cluster compactness, and biological fidelity.

Figure 1 compares the UMAP projections of cell embeddings obtained from hSNMF, NSF, and RASP. The proposed hSNMF method (Fig. 1a) produces compact, well-separated clusters with smooth boundaries, indicating both geometric cohesion and clear transcriptional differentiation. In contrast, the non-spatial NSF baseline (Fig. 1b) yields elongated, overlapping clusters lacking spatial organization, consistent with its low Silhouette scores and negative Moran’s I . The RASP embedding (Fig. 1c) preserves some global structure but exhibits partial mixing between clusters. Overall, hSNMF yields the most coherent and separable manifolds, aligning with its superior quantitative performance in Table 1.

5. CONCLUSION

We presented two spatially regularized extensions of nonnegative matrix factorization (NMF) for dimensionality reduction in spatial transcriptomics. The proposed Spatial NMF (SNMF) introduces spatial smoothness through local graph diffusion of cell factors, providing a simple yet effective way to enhance tissue coherence in low-dimensional embeddings. Building on this, the Hybrid Spatial NMF (hSNMF) (implemented using a contact–radius hybrid graph) integrates both spatial proximity and transcriptomic similarity within a unified clustering framework. Experiments on a Xenium cholangiocarcinoma dataset demonstrate that SNMF and hSNMF substantially improve spatial compactness (low CHAOS, high Moran’s I) and biological consistency (higher CMC and enrichment) compared to non-spatial baselines. The hybrid formulation achieves the most balanced trade-off between geometric and molecular coherence, yielding spatially contiguous yet biologically interpretable and separable clusters. Future work will extend this framework to incorporate multi-scale spatial graphs and compare against deep generative spatial models.

6. COMPLIANCE WITH ETHICAL STANDARDS

This retrospective study utilized de-identified Xenium-based spatial transcriptomics data from patients evaluated for cholangiocarcinoma at the MD Anderson Cancer Center (MDACC). The study protocol was approved by the MDACC Institutional Review Board (IRB). Given the retrospective nature and use of de-identified data, the requirement for informed consent was waived per IRB determination.

7. ACKNOWLEDGEMENT

The work was, in part, supported by STRIDE funding to METI from MD Anderson Cancer Center. We thank the cholangiocarcinoma clinical and pathology group at MD Anderson Cancer Center for providing the tissue microarrays. This project was also supported by the Center for Transformative Pathology and Health (CTPH) under award UM1TR004539. The authors declare that they have no relevant financial or non-financial conflicts of interest.

8. REFERENCES

- [1] Caitlin Schroyer and Shanshan Zhou, “Spatial transcriptomic study of the tumor microenvironment in hnscc,” *Cancer Research*, vol. 84, no. 6_Supplement, pp. 3652–3652, 2024.
- [2] Amanda Janesick, Robert Shelansky, Andrew D Gottscho, Florian Wagner, Stephen R Williams, Morgane Rouault, Ghezal Beliakoff, Carolyn A Morrison, Michelli F Oliveira, Jordan T Sicherman, et al., “High resolution mapping of the tumor microenvironment using integrated single-cell, spatial and in situ analysis,” *Nature communications*, vol. 14, no. 1, pp. 8353, 2023.
- [3] Lulu Shang and Xiang Zhou, “Spatially aware dimension reduction for spatial transcriptomics,” *Nature communications*, vol. 13, no. 1, pp. 7203, 2022.
- [4] Sophia K Longo, Margaret G Guo, Andrew L Ji, and Paul A Khavari, “Integrating single-cell and spatial transcriptomics to elucidate intercellular tissue dynamics,” *Nature Reviews Genetics*, vol. 22, no. 10, pp. 627–644, 2021.
- [5] Shuangsang Fang, Bichao Chen, Yong Zhang, Haixi Sun, Longqi Liu, Shiping Liu, Yuxiang Li, and Xun Xu, “Computational approaches and challenges in spatial transcriptomics,” *Genomics, proteomics & bioinformatics*, vol. 21, no. 1, pp. 24–47, 2023.
- [6] Jun Du, Yu-Chen Yang, Zhi-Jie An, Ming-Hui Zhang, Xue-Hang Fu, Zou-Fang Huang, Ye Yuan, and Jian Hou, “Advances in spatial transcriptomics and related data analysis strategies,” *Journal of translational medicine*, vol. 21, no. 1, pp. 330, 2023.
- [7] Chengwei Zhong, Kok Siong Ang, and Jinmiao Chen, “Interpretable spatially aware dimension reduction of spatial transcriptomics with stamp,” *Nature Methods*, vol. 21, no. 11, pp. 2072–2083, 2024.
- [8] Iivari Kleino, Paulina Frolovaité, Tomi Suomi, and Laura L Elo, “Computational solutions for spatial transcriptomics,” *Computational and structural biotechnology journal*, vol. 20, pp. 4870–4884, 2022.
- [9] Daniel D Lee and H Sebastian Seung, “Learning the parts of objects by non-negative matrix factorization,” *nature*, vol. 401, no. 6755, pp. 788–791, 1999.
- [10] F William Townes and Barbara E Engelhardt, “Non-negative spatial factorization,” *arXiv preprint arXiv:2110.06122*, 2021.
- [11] Ian K Gingerich, Brittany A Goods, and H Robert Frost, “Randomized spatial pca (rasp): a computationally efficient method for dimensionality reduction of high-resolution spatial transcriptomics data,” *Research Square*, pp. rs-3, 2025.
- [12] Yidi Sun, Lingling Kong, Jiayi Huang, Hongyan Deng, Xinling Bian, Xingfeng Li, Feifei Cui, Lijun Dou, Chen Cao, Quan Zou, et al., “A comprehensive survey of dimensionality reduction and clustering methods for single-cell and spatial transcriptomics data,” *Briefings in Functional Genomics*, vol. 23, no. 6, pp. 733–744, 2024.
- [13] Jiyuan Yang, Lu Wang, Lin Liu, and Xiaoqi Zheng, “Graphpca: a fast and interpretable dimension reduction algorithm for spatial transcriptomics data,” *Genome Biology*, vol. 25, no. 1, pp. 287, 2024.
- [14] Md Ishtyaq Mahmud, Veena Kochat, Suresh Satpathi, Jagan M. R. Dwarampudi, Kunal Rai, and Tania Banerjee, “Benchmarking dimensionality reduction techniques for spatial transcriptomics,” in *Proceedings of the 16th ACM International Conference on Bioinformatics, Computational Biology, and Health Informatics (BCB '25)*, Philadelphia, PA, USA, October 2025, pp. 1–10, <https://doi.org/10.1145/3765612.3767237>.
- [15] Samuel L. Wolock, Romain Lopez, and Allon M. Klein, “Scrublet: Computational identification of cell doublets in single-cell transcriptomic data,” *Cell Systems*, vol. 8, no. 4, pp. 281–291.e9, 2019.